CONF-801102--18

LA-UR-80-1844

TITLE: DE-ENTRAINMENT ON VERTICAL ELEMENTS IN AIR DROPLET CROSS FLOW

AUTHOR(S): John C. Dallman
Walter L. Kirchner

MASTER

SUBMITTED TO: ASME Winter Meeting (Chicago, November 16-21, 1980).

los alamos
scientific laboratory
of the University of California
LOS ALAMOS, NEW MEXICO 87545

An Affirmative Action/Equal Opportunity Employer

Form No. 836 R2
St. No. 2629
1/78

DEPARTMENT OF ENERGY
CONTRACT W-7405-ENG. 36

DE-ENTRAINMENT ON VERTICAL ELEMENTS IN AIR DROPLET CROSS FLOW

by

John C. Dallman and Walter L. Kirchner

ABSTRACT

De-entrainment phenomena on vertical elements in air-water droplet cross flow are generated using a horizontal array of water spray nozzles and a draft-induced wind tunnel. These conditions are used to obtain experimental values of the de-entrainment efficiency of isolated elements (25.4-, 63.5-, and 101.6-mm-diam cylinders and a 76.2-mm-square tube), and of an array of 101.6-mm-diam cylinders. A flow model is developed that extrapolates the de-entrainment efficiency of isolated elements through the use of a correlation for the "interference effect" to predict the efficiency of large arrays of similar elements. This simple model is shown to provide a good prediction of the de-entrainment efficiency of arrays in terms of the efficiency of an isolated element.

NOMENCLATURE

A_T	=	Total cross-sectional area at section of infinite array
A_{GN}	=	Total cross-sectional area of gaps in row N of section defining A_T
D	=	Vertical element diameter
F	=	Fraction of air-droplet jet intercepted by a row
Re	=	Reynolds number
STk	=	Stokes number
U	=	Velocity
We	=	Weber number
β	=	Diameter-to-pitch ratio
η	=	De-entrainment efficiency

SUBSCRIPTS

a	=	Air
d	=	Droplet
G	=	Gap between elements
I	=	Isolated element
N	=	Row number in an array
μ	=	Dynamic viscosity
ρ	=	Density
T	=	Total

INTRODUCTION

The importance of gas-droplet flows has increased with the need for greater overall efficiency in industrial processes, power generation, and due to its role in nuclear reactor safety. Although considerable effort has been expended studying the formation of gas-droplet flows (entrainment), little effort has been expended on the de-entrainment (droplet removal) of the droplet field, with the possible exception of the special cases of steam drying and aircraft icing. In

site water supply resulted in minor uncontrolled spray fluctuations. These equipment limitations resulted in the isolated element de-entrainment measurements being repeatable within ± 10 per cent. Of the measurements presented, only those in Fig. 3 and the measurements in Fig. 4 with Weber number less than 230 were obtained using this facility.

The second facility allowed for greatly improved measurement precision and repeatability. Air flow rates are controlled by an electronically operated vortex damper system resulting in highly reproducible conditions with major fluctuations (due to gusty winds) less than 5 per cent. Use of a stable water recirculation system allowed for reproducible spray conditions within about 1 per cent. Measurements using this facility were easily repeatable within about a 5-per cent band. Data presented in Fig. 4, with Weber number greater than 250, and all that presented in Figs. 5, 6, and 7 were obtained using this facility.

center of the test area.

The wind tunnel in Fig. 1 is operated in an induction mode with air entering a 2.9-m^2 entrance cone, then passing an array of spray nozzles, on to an elliptical contraction section, and finally the test section. After passing through the test section, the mixture enters a liquid separator from which the water is recycled and the air released to the atmosphere.

Water droplets are admitted to the air flow by an array of horizontal spray nozzles located 1.27 m from the start of the test section. These nozzles were purchased from Spraying System Company and provide a spray with a volume median diameter varying from 2650 μm to 2200 μm as the pressure at the nozzle tip is varied from 69 to 275 kPa. The spray array was designed such that total coverage of the test area cross section was obtained even at the highest flow velocities. However, this ensured that at lower flow velocities, some of the droplet spray

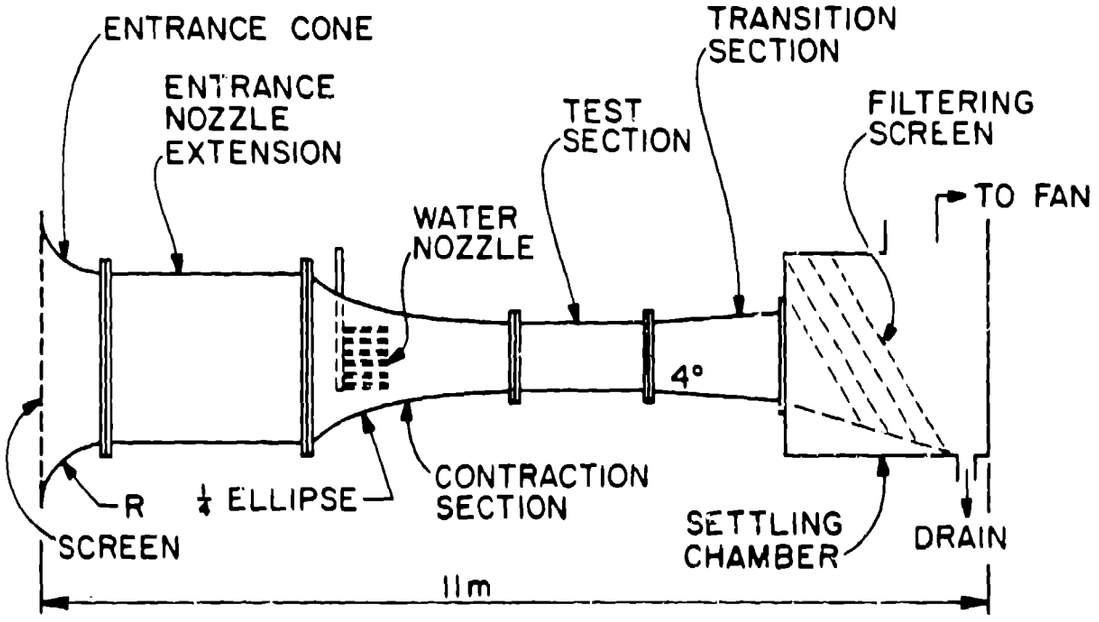

Fig. 1. Wind Tunnel Facility Schematic.

The test area for both facilities is identical and, in fact, is interchangeable. This test area consists of a 0.32-m^2 cross-sectional flow area designed to accommodate a wide variety of shapes and configuration of simulated upper plenum internals. Figure 2 indicates the design of the test section floor and ceiling. It is capable of accommodating a 17-pin "infinite" array of 101.6-mm tubes. For the isolated-element measurements, adapters were fabricated for the smaller diameter or noncylindrical test internals. These measurements were performed with the isolated element at the

local measurement techniques rather than an overall would strike the test section walls before reaching the test elements. This necessitated the use of mass balance technique.

Measurement of De-Entrainment Rates

As the air-droplet two-phase flow strikes a test element placed in the flow stream, some fraction of the droplet field is de-entrained on the element surface and drains as a thin liquid film on approximately the upstream 180° of the surface.(8) The de-entrainment efficiency of an isolated element was

addition to those already mentioned, the removal of droplets from a gas-droplet flow has important applications in the cleaning of industrial gaseous and particulate effluents, abnormal operating conditions involving boiler tubes, and certain events in nuclear reactor components during atypical operating conditions.

The focus of this study is steam-droplet flow in geometries typical of the upper plenum of a pressurized water reactor (PWR) during the course of a loss-of-coolant accident (LOCA). The droplet flow, generated from the core region during the reflood stage of the accident, may either de-entrain on the upper plenum internals or be carried out a hot leg, where it may vaporize in the steam generators. Significant water de-entrainment in the upper plenum results in a potential reduction of the steam binding problem (which impedes core reflood by raising the system back pressure). In addition, the de-entrained water may collect in the upper plenum and drain into the relatively cooler core channels, resulting in an increase in core cooling.

This paper presents the results of a study of de-entrainment phenomena using simulated reactor upper plenum internals in air-water droplet cross flow. Studies of de-entrainment phenomena were carried out using a horizontal wind tunnel and a specially designed water spray system. Measurements of the air-droplet flow characteristics and the de-entrainment efficiencies of various shapes and sizes of isolated simulated internals are presented.

In addition, measurements of the de-entrainment efficiency of a staggered array of 101.6-mm cylinders are presented for superficial velocities of 7 and 14 m/s. Based on geometric considerations and an "interference effect" (enhanced de-entrainment of an array element compared to that of an isolated element), a predictive equation is developed that relates the isolated de-entrainment efficiencies to those of an array of cylinders.

MECHANICS OF DE-ENTRAINMENT

Much of the early theoretical work related to droplet or particle separation from a gas stream by isolated elements was concerned with the filtration of aerosols ($d < 10\mu$). There are three basic mechanisms of aerodynamic capture of aerosols: diffusion, particle interception, and inertial impaction. For the water droplet size expected in a PWR upper plenum during reflood (volume median ~ 1000 μm)(1) only the inertial impaction mechanism is of importance. In this model of droplet motion, as a gas stream approaches a body placed normal to the stream, the fluid streamlines spread around the body. The exact streamline configuration depends upon the body shape, gas velocity, and fluid properties of the gas. Drops traveling in the gas stream, due to inertial effects, tend not to follow the curvature of the streamlines, but hurtle across and impact on the obstructing surface.

Brun, et al.,(2) have solved the equations of motion for inertial impaction of a water drop traveling at the free stream conditions in potential flow past a vertical cylinder. The resulting "S"-shaped curves indicate a strong dependence of impaction efficiency on a Stokes number. For Stokes numbers in the range of this study, $1000 < Stk < 10000$, the impaction efficiencies are nearly 100 per cent. This indicates that the disturbance generated by the element in the flow stream will have little or no effect on the path of the approaching droplet field (except on the smallest drops in the droplet field; however, these will contain only a small fraction of the total mass). Thus, large droplets on a path of interception with an element eventually collide with that element.

High-speed motion pictures (3) (4000 frames/s) of 10 m/s air-droplet cross flow striking a 25-mm cylinder have indicated at least four very complicated mechanisms reducing de-entrainment efficiency from that of the inertial impaction efficiency: 1) incoming droplet breakup upon impact with a dry surface and subsequent droplet fragment entrainment, 2) incoming drops striking a thin film with subsequent crater formation and back splash of satellites and fragments of the original drop, 3) incoming drops impacting a surface at a glancing angle and bouncing free of the surface, possibly removing a portion of the film, and 4) hydrodynamic re-entrainment of the liquid film by the air stream.

Observation of the high-speed movies indicated that the dominant mechanism appears to be droplet splashing upon impact with the thin water film. Although fundamental studies, including both experimental and theoretical investigations, have been carried out by Macklin and Metaxes,(4) Mondy,(5) Jayaratne and Mason,[6] Harlow and Shannon,(7), these studies have all been performed using stagnant liquid layers. To maintain a stable stagnant film, the film must of necessity be rather deep, in the range of 2 mm. In contrast, recent measurements (3) of the average film thickness on a 101.6-mm cylinder in air-droplet cross flow have indicated values ranging from 0.1 to 0.6 mm. Consequently, application of the results of these droplet splashing studies to de-entrainment phenomena on vertical elements has been, to date, unsatisfactory.

EXPERIMENTAL FACILITY

The steam-droplet flows in the upper plenum of a light-water pressurized reactor have been simulated using air-droplet flows in a draft induction wind tunnel. Water droplets are admitted by sprays placed in the wind tunnel parallel to the incoming air stream. This air-droplet mixture is then allowed to flow across various size and shape structures designed to simulate the internal elements of the reactor upper plenum. Measurements were made of the mass of droplets impacting per unit cross-sectional area of the structure, as well as the total liquid draining from the structure. The main interest being the ratio of these two quantities, the de-entrainment efficiency, as a function of the pertinent hydrodynamic and geometric variables. Two different wind tunnel facilities were used for this study. The bulk of the isolated-element de-entrainment measurements was obtained with a facility that is described in detail in Ref. 3. Some of the isolated-element measurements and all the multiple-element measurements were obtained in the wind tunnel facility shown in Fig. 1. This wind tunnel design significantly increased the maximum air and water flow rates as well as eliminated several minor design flaws of the original facility.

In the original de-entrainment facility, due to equipment limitations, air flow reproducibility was about $\pm$ 10 per cent. In addition, poorly regulated

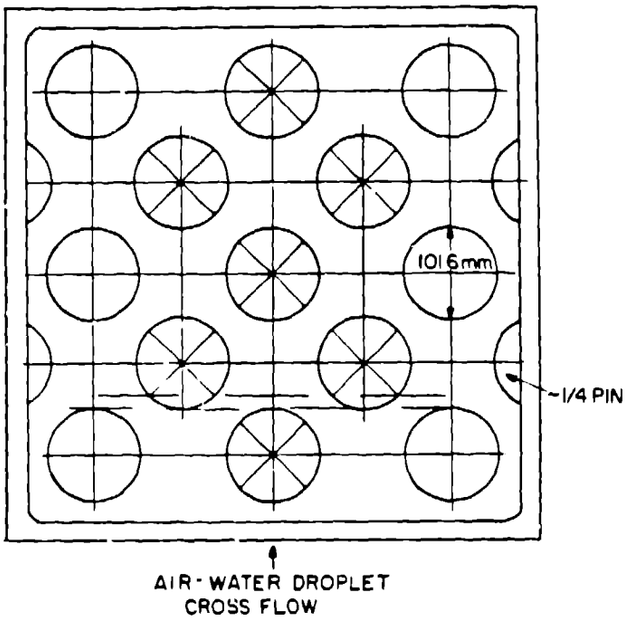

Fig. 2. Schematic of the 101.6-mm-diam array.

determined by measuring the volumetric rate of flow in the draining film and the volumetric rate at which the droplet flow impacted on the element. The ratio of these two measurements represents the de-entrainment efficiency of the element. (This technique is documented in greater detail in Ref. 3.) The large number of cylinders in the array investigation made it impractical to measure directly the draining liquid film or the impacting droplet mass flow rate. For these purposes a large Pitot rake was fabricated that has a vertical dimension of 19 mm and a horizontal dimension of 446 mm, or approximately 80 per cent, of the test area width. The Pitot rake was centered in the test section, allowing 56 mm between the rake edges and the test section walls. This was done to reduce the influence of any local flow anomalies near the walls. The Pitot rake was connected to a traversing mechanism that moves the rake from test area top to bottom in a continuous manner. The rake was positioned vertically at 25.4-mm ± 1.6-mm intervals where the droplet mass flow was measured. This profile was then integrated to give the total droplet mass flow at the axial location of the measurement. In addition, the Pitot rake can be positioned along the wind tunnel axis at intervals equal to the distance between rows in the array, but the position is not limited to these intervals.

The amount of liquid de-entrained by a given row is then the difference between the integrated mass profile in front of the row of elements and that behind the row. This measurement was repeated for each of the five rows. In a similar manner, the de-entrainment efficiency of the array can be determined by measuring the droplet mass entering the array and that exiting from the array. This technique does not separate such integrated effects as gravitational settling or droplet field angular velocity.

EXPERIMENTAL RESULTS

Isolated Internal De-Entrainment Rates

A convenient way to characterize the liquid de-entrainment on objects of differing shape is to measure the rate of liquid de-entrainment per unit projected cross-sectional area as a function of the average droplet mass flux. The ratio of these quantities is the isolated-element de-entrainment efficiency, η_I. Sample measurements of the de-entrainment efficiency vs the average droplet mass flux for several different sizes and shapes of isolated elements are shown in Fig. 3. Because the estimated initial droplet velocity is different from that of the air flow, it is shown as a parameter in the figure. The data show only small differences in efficiency for the 25.4-, 63.5-, or 101.6-mm cylindrical tubes at mass flux rates above 2 kg/m^2 s; however, the 76.2-mm square tube appears to be slightly more efficient than the cylinders at these higher mass flux rates. Hence, there appears to be only a minor dependence on air velocity, droplet mass flow rate, tube diameter, and droplet velocity for average liquid mass flux rates between 2 and 15 kg/m^2 s (the highest value measured in this study) and air velocities less than 14 m/s.

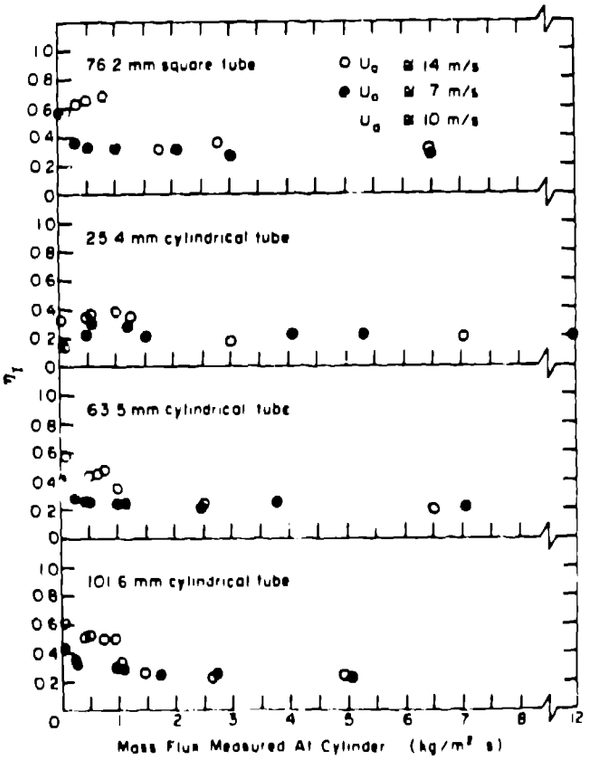

Fig. 3. Effect of droplet mass flux on isolated element de-entrainment efficiencies.

At the lowest mass flux rates in Fig. 3, the water is distributed over the forward half of the cylinder in a discontinuous manner. At these flow rates the water collects in small pools on the surface then drains through rivulets to the floor of the wind tunnel. As the droplet flow rate to the surface increases, these rivulets and pools gradually expand until a thin continuous film forms.

Mondy(5) has reported measurements indicating that droplets are more easily bounced or splattered from a thin water film than from a dry stainless steel plate regardless of the angle of impact. This tends to explain the high efficiencies at low droplet flux rates since a substantial portion of the surface does not have a water film. The apparent maxima or plateau through which the data pass at a mass flux of about 0.5 to 1.0 kg/m^2 s is rather difficult to explain without further study. However, as the flux of droplets to the element surface increases, the rivulets and pools tend to attach and form a continuous film. This film is thinner than the original rivulets or pools and has less mass available at a given location for splattering. However, as the film thickens at higher flux rates, the efficiency again plummets where it appears that the efficiency (and the splashing phenomena) reaches a "deep film" asymptote. Much of this explanation remains specululative due to the difficulty in measuring discontinuous films and due to the visual and qualitative nature of this explanation. These phenomena will be explored in future studies planned as part of this continuing investigation.

In addition to the extensive isolated-element studies at 7 and 14 m/s, a limited number of de-entrainment measurements for air velocities up to 40 m/s are presented in Fig. 4 for the 101.6-mm isolated cylinder. At these higher flow velocities, the de-entrainment efficiency decreases almost linearly with increasing cylinder Weber number, defined as

$$We = \frac{\rho_a U_a^2 D}{\sigma} , \qquad (1)$$

where the subscript a refers to the properties of ambient air, D is the cylinder diameter, and σ is the surface tension. It is speculated that this decrease in de-entrainment is due to the re-entrainment of the draining liquid film and increased sweep out of splashed drops by the air flow.

The linear relationship between the isolated de-entrainment efficiency and the cylinder Weber number is based on dimensional reasoning concerning the entrainment of a liquid film by an air flow. In the opinion of the authors, the use of the cylinder diameter, D, as the length parameter in the Weber number probably overpredicts the effect of cylinder diameter. A better parameter would be the average draining film thickness. As only a few measurements of the film thickness are available, it was not possible to incorporate this parameter in Fig. 4.

Array De-entrainment

Multicylinder array de-entrainment measurements were made using the array configuration shown in Fig. 2 and the Pitot rake system described above.

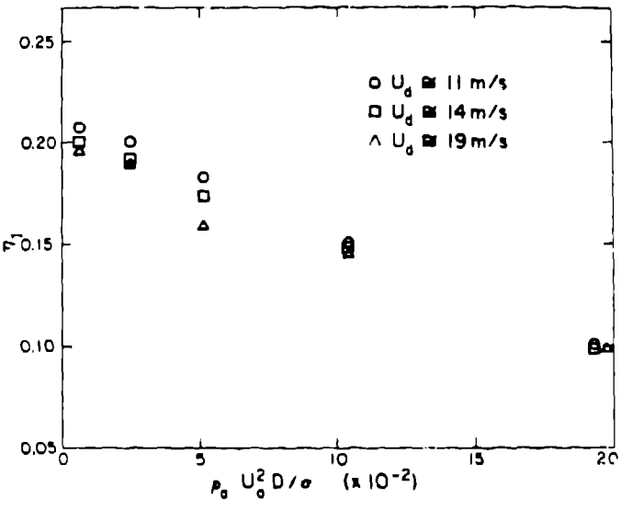

Fig. 4. De-entrainment efficiency of a 101.6 mm-diam cylinder as a function of cylinder Weber Number (for droplet mass flux rates > 2 kg/ms).

The mass rate of droplet flow was measured at the leading edge of a row and approximately 25 mm behind the row with identical flow conditions. The difference of these two measurements is the amount of the droplet field de-entrained by the row; and the array de-entrainment efficiency η_{NA} (where N is the number of rows in the array) is the ratio of this difference to the measured mass flow rate of drops at the leading edge.

The approaching droplet field mass profile was initially peaked at the axis of the tunnel; however, after several rows the profile changed to one with an almost flat profile with only a slight increase from the top to the bottom of the test area (see Fig. 5). The average droplet mass flux for the array measurements varied from about 6.5 kg/m^2 s to 11 kg/m^2 s, corresponding to the upper range of the isolated internals measurements.

Measurements of the de-entrainment efficiency of the array shown in Fig. 2 are presented in Figs. 6 and 7 for superficial air velocities of 7 and 14 m/s, respectively. The array used had a packing density (volume fraction of cylinders) of about 0.39, with individual rows having an average pitch-to-diameter ratio of 0.5.

It is interesting to note that after just three rows of tubes, between 75 and 85 per cent of the incoming droplet mass has been de-entrained. Additionally, over the range of flow conditions in this study, there is a difference of about 6 per cent between the 7 and 14 m/s measurements after the first row. These differences are due to the fact that the internal elements of the array are in an air flow field with a Weber number approximately twice that of the superficial Weber number (250 and 1030, respectively).

An examination of Fig. 4 indicates that there is approximately a 4-per cent difference in the isolated element efficiency over this range of Weber number

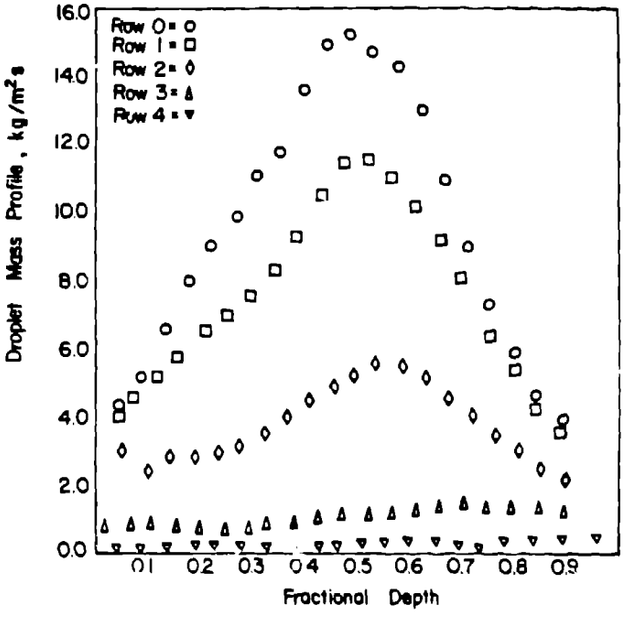

Fig. 5. Droplet mass distribution measured at leading edge of array.

(250 to 1030). In a later section it will be shown that this is sufficient to explain the differences in the array de-entrainment efficiencies.

PREDICTION OF ARRAY DE-ENTRAINMENT EFFICIENCY

As a gas-droplet flow passes through an array of elements, the flow stream tends to form jets or local concentrations of the droplets that exit each row through the gaps between the elements. These "jets" tend to be diffused by local fluid motions as they move toward the next row of elements. Thus, the droplet mass flow rate impinging on the subsequent row is subject to the local flow conditions, the distance to the next row, and the geometric position of the elements of the next row.

If an initially homogeneous air-droplet mixture is flowing through a section of an infinite array of elements with a projected area to the flow of A_T, a total projected area of the gaps between elements for row N of A_{GN}, and F_N the fraction of the air-droplet jet formed in the N-1th row and intercepted by the elements of the Nth row, then an equation for a multirow array can be derived having the following form

$$\eta_{NA} = 1 - \left[1 - \left(\frac{A_T - A_{G1}}{A_T}\right)\eta_1\right]\left[1 - \left(\frac{A_T - A_{G2}}{A_{G1}}\right)F_2\eta_2\right] \cdots \left[1 - \left(\frac{A_T - A_{GN}}{A_{GN-1}}\right)F_N\eta_N\right] \quad . \qquad (2)$$

For a regular array,

$$\beta = \frac{A_T - A_{GN}}{A_T} \quad , \qquad (3)$$

where β is the diameter-to-pitch ratio of the array, and η_N is the de-entrainment efficiency of the elements in the Nth row. In addition, the array in Fig. 2 is staggered with each gap of the N-1th row filled by an element of the Nth row, thus $F_N = 1$.

For a regular array similar to Fig. 2, Eq. (2) reduces to

$$\eta_{NA} = 1 - (1 - \beta\eta_1)\left(1 - \frac{\beta}{1-\beta}\eta_2\right) \cdots \left(1 - \frac{\beta}{1-\beta}\eta_N\right) \quad , \qquad (4)$$

where $\frac{\beta}{1-\beta} < 1$. For cases where $\frac{\beta}{1-\beta} > 1$, the ratio should be set to 1.0. In addition, the diameter-to-pitch ratio for the array of Fig. 2 is very close to 0.5 for the interior rows and 0.55 for the first row; hence, Eq. (4) becomes

$$\eta_{NA} = 1 - (1 - 0.55\eta_1)(1 - \eta_2) \cdots (1 - \eta_N) \quad . \qquad (5)$$

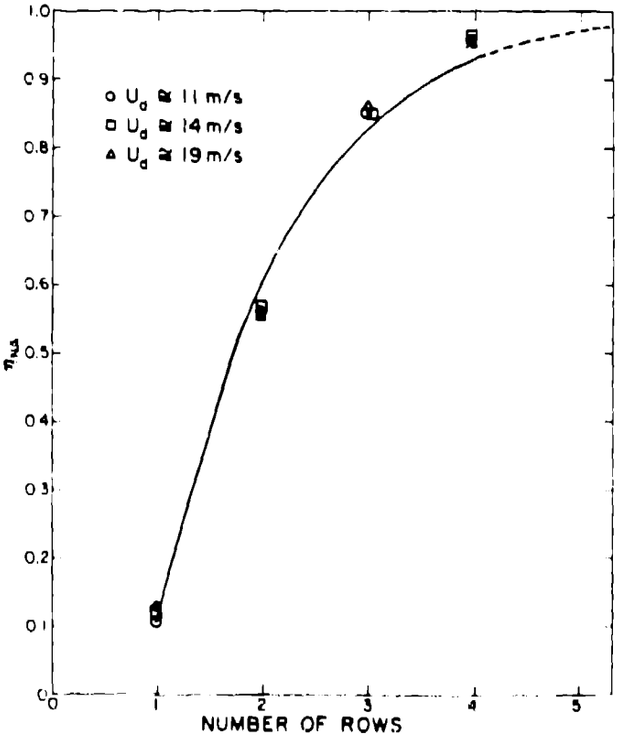

Fig. 6. Array de-entrainment efficiency for arrays of 101.6-mm-diam cylinders with average air velocity at 7 m/s.

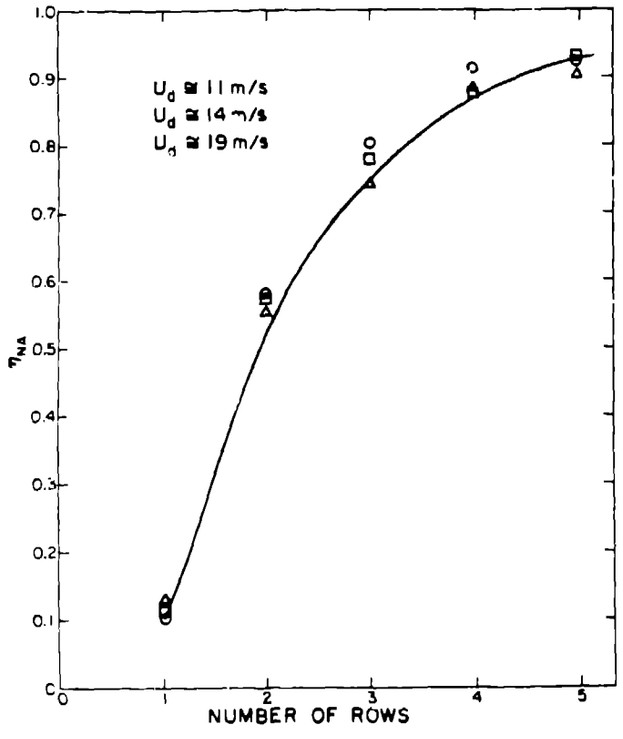

Fig. 7. Array de-entrainment efficiency for arrays of 101.6-mm-diam cylinders with average air velocity at 14 m/s.

It has previously been noticed(9,10) in the filtration of aerosols by impaction that there is considerable disagreement between the efficiences of isolated filter fibers and the efficiency of a fiber in a filter. This phenomena has been called the "interference effect." An empirical correlation, based on filtration measurements, of the efficiency of an element from a row in terms of the diameter-to-pitch ratio, β, and the isolated element de-entrainment efficiency has been proposed by Chen(9) and has the form

$$\eta_N = (1 + 4.5\,\beta^2)\,\eta_I \quad , \qquad (6)$$

where η_N is the de-entrainment efficiency of a row element and η_I is the isolated element de-entrainment efficiency (Chen's measurements included arrays with $\beta \leq 0.32$). Application of Eq. (6) to the case of large drops impacting on 101.6-mm cylinders is difficult to justify; however, it might be expected that there would be strong similarities between the filtration of 10-mm aerosol droplets on 1-mm fibers and the de-entrainment of 1000-μm drops on 100-mm cylinders. Until additional de-entrainment information is available on varied array configurations, it is suggested that Eq. (6) serve as the best available correlation of the "interference effect."

MODEL COMPARISON WITH EXPERIMENTAL RESULTS

Single Row Array

Observation of the single-row array or of the first row of a multirow array has indicated that essentially all of the droplet-cylinder interaction occurs on the upstream 180° of an element surface. Thus, it may be expected, intuitively, that the flow conditions directly upstream (i.e., the superficial flow conditions) would dominate any lateral or downstream effects. This implies that each element of the first row (or single row) acts essentially as an isolated element in cross flow without interference effects.

The isolated element de-entrainment efficiency for the 7 and 14 m/s air velocity cases can be determined from Fig. 4 using the approximated superficial Weber numbers, 64 and 250, respectively. Using the values obtained for η_I in Eq. (5), [Eq. (6) is not used because there is little "interference" in the first row], an excellent prediction of the single-row array measurements results. This can be observed in Figs. 6 and 7.

Thus, the elements of a single row or of a first row of a multirow array can be treated as isolated elements with the upstream superficial flow conditions dominating the de-entrainment process. This is not the case for the latter elements of a multirow array and, as will be seen in the next section, the use of Eq. (6) to determine the interference effect is necessary.

Multirow Array

The application of Eq. (6) requires a value for the isolated-element efficiency, η_I, at the local flow conditions surrounding the array element. This can be obtained by estimating the local cylinder Weber number and referring to Fig. 4.

The first row of the array has been shown to be well described by Eq. (5) using the η predicted from the upstream flow conditions. Interior rows are in a considerably higher air velocity field, in fact, the array of Fig. 2 has a local air velocity about twice the superficial velocity.

Using values of the Weber number for the 7 m/s and 14 m/s superfical velocity cases, (250, 1030), η can be interpolated using Fig. 4. Using these values in Eq. (6) and subsequently in Eq. (5) the results are shown as the solid lines in Figs. 6 and 7.

The predictive line of Eq. (5) in Fig. 7 gives an excellent representation of the array de-entrainment measurement for the 14 m/s superficial velocity case. On the other hand, the prediction of Eq. (5) for the 7 m/s case in Fig. 6 does a good job of representing the one- and two-row arrays, but for the larger arrays appears to systematically underpredict the measurements by about 4 per cent. This discrepancy for large arrays is probably due to the gravitational settling of the drops at low cross flow velocities.

Simple scoping calculations using a drag on a sphere model (~ 1.0 mm diam, 7 m/s superficial velocity) have indicated that for an array similar to that of Fig. 2 the de-entrainment due to gravitational settling could be as high as 2 per cent per row after the first row. However, in the case of steam droplet flows in a pressurized water reactor upper plenum during reflood, the flow will have a vertical velocity component as well as a horizontal component. For this case it would appear that

gravitational settling would be reduced considerably except at the lowest velocities and these probably would not generate dispersed flows.

Although good predictions have resulted from the application of Eq. (5) and (6) along with Fig. 4, caution should be exercised in the general application of these equations to conditions or array geometries greatly differing from those of this study. In addition, at this time there is insufficient information available to truly test Eq. (6) or develop an alternative; hence, results in sparse or very dense arrays may not be well represented by this correlation.

SUMMARY

The isolated element de-entrainment efficiencies for air velocities of 7 and 14 m/s are shown to be strongly dependent upon droplet mass flux rate below 2 kg/m^2 s. Above this value the de-entrainment efficiency is constant up to the limit of this study, 15 kg/m^2 s.

A limited number of isolated de-entrainment efficiency measurements are reported for a 101.6-mm cylindrical element at air velocities up to 40 m/s (We = 2000). These measurements indicate an almost linear decrease in de-entrainment efficiency with increasing air velocity, from 20 per cent at 7 m/s air velocity to 10 per cent at 40 m/s. In addition, there is a slight decrease in efficiency with increasing droplet velocity.

De-entrainment measurements of the array of 101.5-mm-diam cylindrical elements, used in this study, have shown a high efficiency for droplet removal. The first three rows of this array removed more than 75 per cent of the incoming droplet mass, at superficial air velocities up to 14 m/s.

Preliminary predictive relations have been developed, using geometric considerations and a correlation for the "interference effect," which show that the multielement array de-entrainment measurements of this study are reasonably predicted in terms of the isolated element de-entrainment measurements.

Studies are under way to determine the efficiency of this array at significantly higher superficial air velocities and droplet mass flow rates. In addition, similar measurements are planned for different array configurations and element diameters. These measurements will aid in the fundamental goal of developing of generalized predictive relations for array de-entrainment efficiency.

REFERENCES

1. R. S. L. Lee, J. R. Srinivasan, and S. K. Cho, "Droplet Entrainment Studies of Dispersed Flow Through Tie Plates in LOCA by LDA Method," presented at the Seventh Water Reactor Safety Research Information Meeting, National Bureau of Standards, Gaithersburg, MD, Nov. 5-9, 1979.

2. R. J Brun, W. Lewis, P. J. Perkins, J. S. Serafini, "Impingement of Cloud Droplets on a Cylinder and Procedure for Measuring Liquid-Water Content and Droplet Sizes in Supercooled Clouds by Rotating Multicylinder Method," NACA 1215 (1955).

3. J. C. Dallman and W. L. Kirchner, "De-entrainment Phenomena on Vertical Tubes in Droplet Cross Flow," Los Alamos Scientific Laboratory report, LA-8316-MS (1980).

4. W. C. Macklin and G. J. Metaxes, "Splashing of Drops on Liquid Layers," J. Appl. Phys. 47, 3963 (1976).

5. L. Mondy, from lecture entitled, "Droplet Splashing on Dry Surfaces and in Liquid Pools," Los Alamos Scientific Laboratory (Summer 1979).

6. O. W. Jayaratne and B. J. Mason, "The Coalescence and Bouncing of Water Drops at an Air/Water Interface," Proc. Roy Soc., London A 280, 545 (1964).

7. F. H. Harlow and J. P. Shannon, "Distortion of a Splashing Liquid Drop," Science 157, 547-550 (1967).

8. J. C. Dallman, W. L. Kirchner, and V. S. Starkovich, "De-entrainment Phenomena from Droplet Cross Flow in Vertical Bundles," Trans. Am. Nucl. Soc. 30, 381 (1978).

9. C. Y. Chen, "Filteration of Aerosols by Fibrous Media," Chem. Rev. 55, 595 (1955).

10. C. N. Davies, "The Separation of Airborne Dust and Particles," Proc. Inst. Mech. Engrs. (London) B1, 185 (1952).